

# Orange2013



## Team Member

Ryosuke Amano(SE,Master)  
Naruhito Moriyama(SE,Master)  
Kentaro Ueno(SE,Master)  
Hironobu Kariya(SE,Master)  
Tomoya Yoshida(SE,Master)  
Hideyuki Saito(SE,Master)  
Kazuki Ito(SE,Master)  
Mikito Takahashi(EE,Senior)  
Yoshitaka Fukuda(EE,Senior)  
Shinnosuke Tokuda(EE,Senior)

Faculty of Science and Engineering, Hosei University 3-7-2 Kajinocho Koganei, Tokyo 194-8584, Japan

E-mail; ikko@hosei.ac.jp

## Faculty Advisor Statement

I hereby certify that the engineering design on Orange2013 was done by the current student team and has been significant and equivalent to what might be awarded credit in a senior design course.

Signed

*Kazuyuki Kobayashi*  
Prof. Kazuyuki Kobayashi

Date

*April 30, 2013*  
April 30, 2013

Prof. Kajiro Watanabe

Prof. Kaoru Suzuki

Prof. Kazuyuki Kobayashi

## 1. Introduction and innovation

The Autonomous Robotics Laboratory (ARL) team of Hosei University presents Orange2013 as an entry in the 2013 Intelligent Ground Vehicle Competition (IGVC). In the 2012 IGVC, we were placed second overall, third in the Auto-Nav challenge, and second in the JAUS challenge. Building on our previous success, we have redesigned Orange2013 to account for the new rule changes of the Auto-Nav challenge, both for the basic course and advanced course with obstacles, of the 2013 IGVC. In Table 1, we summarize the requirements and solutions that must be developed to address each challenge.

**Table 1. Requirements & Solutions**

		Auto-Nav Challenge (Basic / Advance)	JAUS Challenge
<b>Requirement</b>		<ul style="list-style-type: none"> <li>• Sinusoidal curve course tracking</li> <li>• Avoid sideswipe / obstacle touch.</li> <li>• The vehicle has to deal with complex obstacles including switchbacks and center islands, dead ends, traps, and potholes.</li> <li>• Recognize flag shape and flag color.</li> </ul> 	<ul style="list-style-type: none"> <li>• Develop sophisticated JAUS software that can handle complex JAUS message combination.</li> <li>• Shorten waypoint navigation time.</li> <li>• Reduce computational load for JAUS message interpretation to faster control of vehicle.</li> </ul>
<b>Solution</b>	<b>Software</b>	<ul style="list-style-type: none"> <li>• Develop stable lane following algorithm.</li> <li>• Develop new collision avoidance algorithm that includes zero-radius turn and incremental robust map generation to detect dead end and switch back.</li> </ul>	<ul style="list-style-type: none"> <li>• Optimize JAUS interpretation software.</li> <li>• Employ intelligent path planning algorithm to generate time-optimal path.</li> </ul>
	<b>Hardware</b>	<ul style="list-style-type: none"> <li>• Employ emergency collision avoidance system.</li> <li>• Employ new omni-directional camera to recognize flag shape and flag color.</li> </ul>	<ul style="list-style-type: none"> <li>• Microcontroller based new JAUS protocol converter is developed for gyro, LRF and vehicle controller.</li> </ul>
		<ul style="list-style-type: none"> <li>• Employ 3D LRF module to recognize various shapes of obstacles including construction barrels, fences and certain other obstacles.</li> </ul>	
		<ul style="list-style-type: none"> <li>• To enhance moving stability at fast speed, payload storage space is allotted at lowered part of vehicle that achieve lower center of gravity in comparison to last year's vehicle.</li> <li>• To prevent electrical trouble under severe environment change such as heat, dust, and rain, we redesigned electrical housing box.</li> </ul>	

## 2. Design process and team organization

### 2.1 Design process

Rapid troubleshooting and preparing several alternative solutions to common problems are important factors for success in IGVC. To find many alternative solutions for vehicle failures, we apply the new failure mode, effects, and criticality analysis (FMECA) design process, which is suitable for designing autonomous vehicles.

According to the FMECA design process, we build a table containing the critical failures of each vehicle and assign to each failure an impact number. The failure impact numbers were decided in team meeting discussions. In Table 2, we preset the developed FMECA table. Using the occurrence number and effect number of each failure (both effects and occurrences are assigned numbers between 1 and 4; 1: no problem, 2: low risk, 3: high risk, and 4: catastrophic.), we compute the criticality of each failure as follows:

$$\text{criticality} = \text{effect}^{1.5} \times \text{occurrence}$$

**Table 2. FMECA table developed for Orange2013**

No	Item	Function	Failure mode	Cause of failure	Occur	Effect	Criticality	Improving	Occur	Effect	Criticality
1	sensors	Receive environment	Vibration	Dividing	3	4	24	Lowering center of gravity	1	1	1
2	Payload	Baggage		Tremor of payload	4	3	20.7	Develop case of payload	2	1	2
3	Vehicle	Moving	Impact	Slow processing	4	3	20.7	Emergency system	1	1	1
4	Circuit	Supply power, etc.	Short	Rain	2	4	16	Develop circuit box	1	2	2.8
5	3DLRF	Obstacle detection	Non-obstacle detection	Difference of angle	4	2	11.3	Change to servo	1	1	1

## 2.2 Team organization

Our team consists of seven graduate and three undergraduate students. In Table 3, we show how our team is divided into subteams, and the responsibilities and objectives assigned to each subteam. To improve the capabilities of Orange2013, each subteam was assigned a major objective.

**Table 3. Team responsibilities and objectives**

Team name	Part	Objective
<b>Hardware team</b>	Manufacture of vehicle CAD drawing	Reduce vibration and increase the moving stability
<b>Electric team</b>	Circuit design, control sensors Developing power supply system	Create a JAUS-compliant sensor module for each sensor component
<b>Software team</b>	Programing, algorithm design Improving algorithm	Optimize software to minimize reaction time and handle complex obstacle courses

The major objective of each subteam for this year's competition is summarized as follows:

- 1) The mechanical team aims to reduce vibration and increase the moving stability.
- 2) The electrical team aims to create a JAUS-compliant sensor module for each sensor component.
- 3) The software team aims to optimize software to minimize reaction time and handle complex obstacle courses.

Overall, this year, the team members worked over 1400 person-hours on improving Orange2013.

### 3. Mechanical design

On the basis of last year's results, we decided that we need to address the vibration problem caused when driving at high speeds over rough ground or on a slope. We addressed the vibration problem by applying the FMECA design process. By analyzing the obtained results, we concluded that we should rearrange the weight distribution of the vehicle and move the center of gravity lower by introducing a storage space for payload. In Fig. 1, we present a three-dimensional (3D) CAD model of the redesigned Orange2013. By using the 3D CAD software package Autodesk Inventor 2011, we were able to rapidly make significant changes to the design.

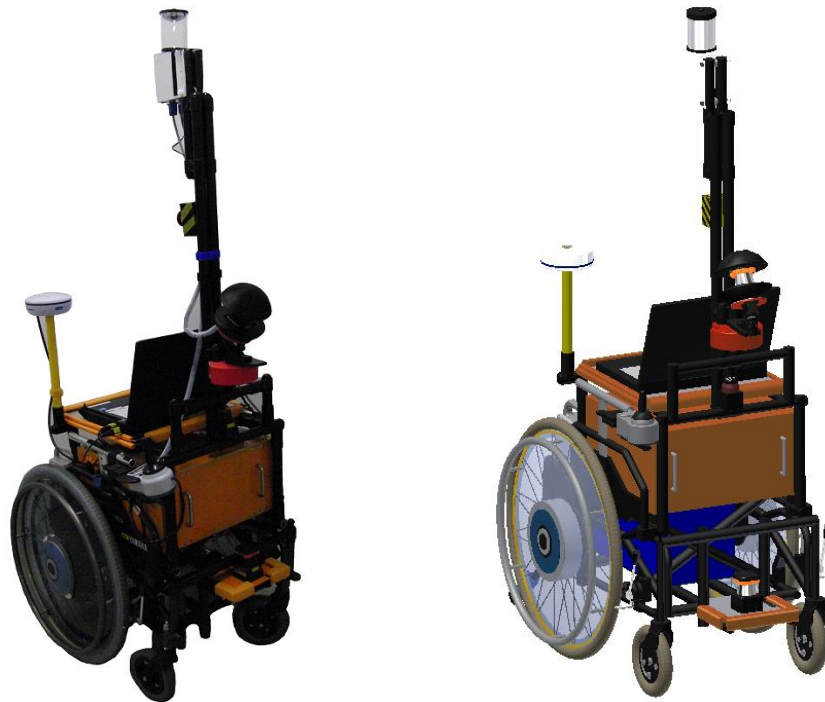


**Fig. 1 Photo and CAD model of Orange2013**

### 3.1 Chassis

Similar to last year, we used the YAMAHA electric wheelchair (JW-Active) as the basic chassis. The main difference in last year's design is that we arranged the components to lower the center of gravity and stabilize the vehicle at high speeds. We lowered the center of gravity by placing the laptop computer on the seat of the wheelchair and introducing a payload storage space, as shown in Fig. 2.

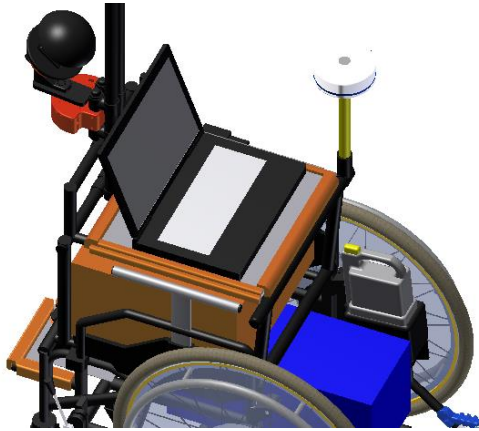


Fig. 2 (a) Placement of laptop computer

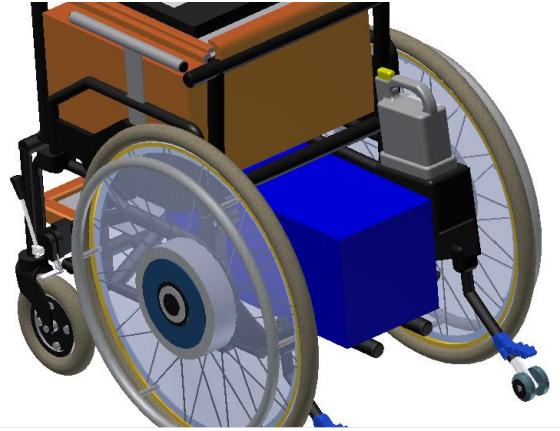


Fig. 2 (b) Payload storage space

### 3.2 Electrical housing box

We redesigned the electrical housing box due to the new placement of the laptop computer, the introduction of the payload storage space, and the need to prevent electrical problems caused by environmental factors such as heat, rain, and dust. In Fig. 3, we illustrate this year's electrical housing box.

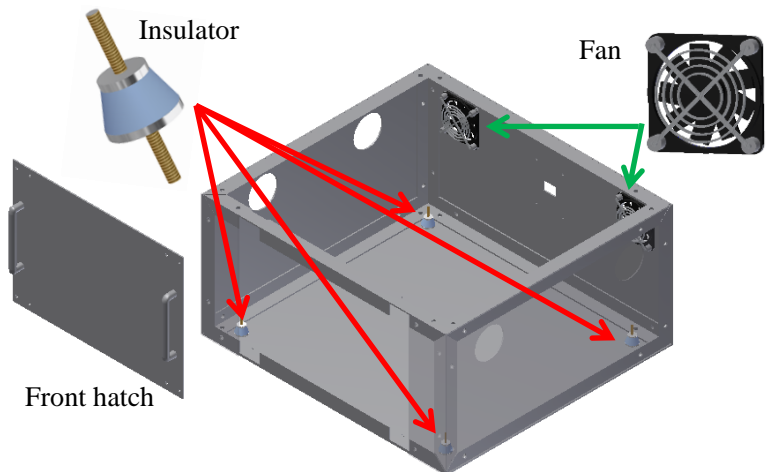


Fig. 3 This year's electrical housing box

### 3.3 Using a new 3D LRF module for 3D obstacle detection

To improve obstacle identification, we developed a new 3D laser range finder (LRF) module that recognizes the three-dimensional shapes of obstacles. The new 3D LRF module has a horizontal and vertical view angle of 270° and 60°, respectively. Instead of the DC motor control system used last year, this year we employed a servo motor system that rotates the 3D LRF module accurately.

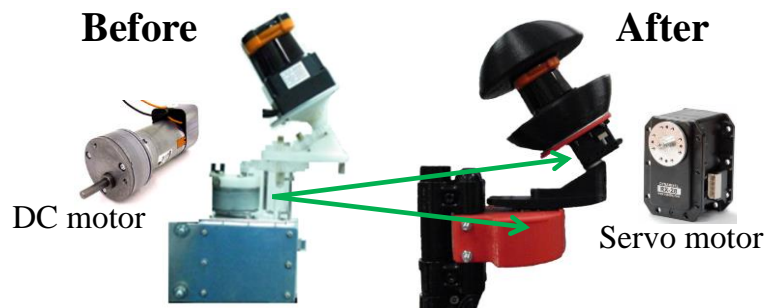


Fig. 4 Differences between last year and this year's 3D LRFs

## 4. Electrical Design

### 4.1 Power system and signal processing

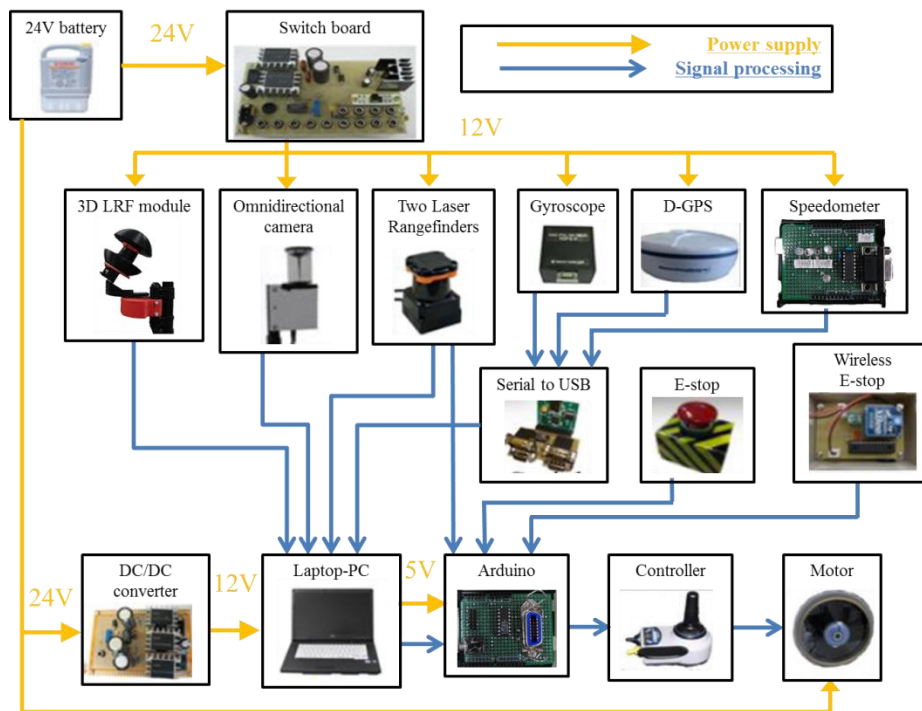
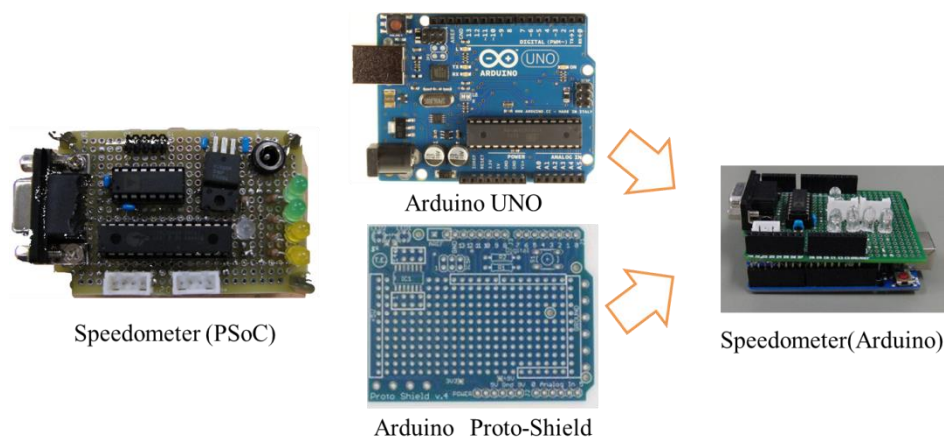


Fig. 5 Power supply system and signal processing

In Fig. 5, we present a schematic diagram depicting the power and signal flows. The main power supply of the vehicle and other peripheral devices is a nickel–metal hydride battery. To prevent damage due to short circuits, we connected the power supplies of the sensors and laptop computer through a polyswitch protected DC/DC converter. In addition, depending on the required voltage for each sensor, we used power supply jacks of different sizes that cannot connect with different plugs. As shown in Fig. 6, to minimize circuit problems caused by hand soldering, we replaced the hand-soldered PSoC board used last year with a readymade Arduino board with a ProtoShield board. In last year’s design, the laptop computer controlled the vehicle by gathering and processing environmental information acquired from sensors. In this year’s design, instead of using the laptop computer to control the vehicle, we perform collision avoidance by connecting a small LRF to the Arduino board.



**Fig. 6 Differences between last year’s PSoC speedometer and this year’s Arduino-based speedometer**

## 4.2 Safety

To achieve stable and safe vehicle navigation, we introduced new emergency collision avoidance and emergency stop systems.

### 1) New emergency collision avoidance system

To prevent obstacle collision, we developed a new emergency collision avoidance system using an Arduino microcontroller. Fig. 7 represents the developed emergency collision avoidance system. By employing the Arduino microcontroller with an external USB shield board that is directly connected to the LRF, the new emergency collision avoidance system enables rapid responses.

### 2) Emergency stop system

For safety purposes, Oragne2013 is equipped with two different types of emergency stop systems (E-Stop and wireless E-Stop) and a safety light. E-stop is placed two feet above ground, at the center rear of the vehicle. This year, we redesigned the wireless E-stop. In particular, to reduce development time and circuit wiring, instead of using the PSoC–Xbee microcontroller, we used the Arduino–Xbee microcontroller. According to the specification sheet, the maximum wireless communication range of Xbee is 33 m. To enhance the visibility of the navigation mode light, we wrapped the central pole of the vehicle with an LED ribbon. When the vehicle is in the autonomous mode, the LED ribbon emits a stable (turn on) light. Conversely, when the vehicle is in the manual mode, the LED ribbon emits a flashing light.

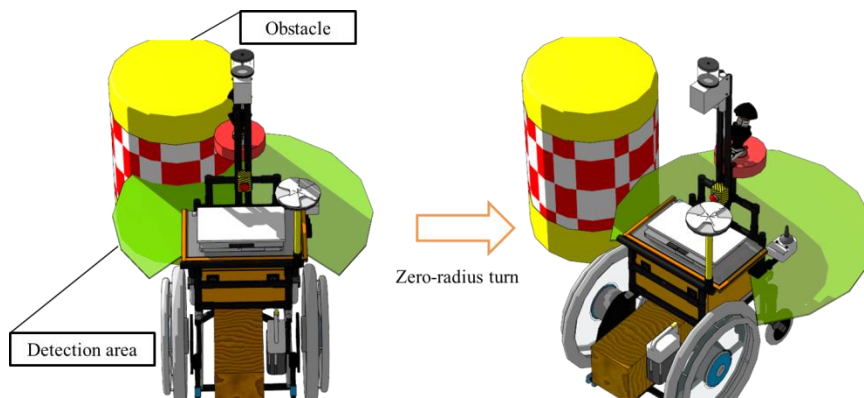


**Fig. 7 Emergency collision avoidance system**

### 4.3 Computer system

The main controller of the vehicle is a laptop computer (FUJITSU LIFEBOOK A561/C) running Microsoft Windows 7 Professional, with a 2.60-GHz Intel Core i5 processor and an 8 GB memory. All sensor signals used to obtain environmental information are transmitted via USB cables and/or an Ethernet connection. To reduce the computational burden of the main controller, Orange2013 employs several additional microcontrollers that perform various tasks.

### 4.4 Sensors

In Table 4, we list the sensors installed on Orange2013. Using the FMCEA design process, we employed six sensors for obtaining environmental and positional information.

**Table 4. List of sensors installed on Orange2013**

Sensor	Detection	Specification
3D LRF module 	*Obstacles	HOKUYO UTM-30LX with roundly swinging mechanism *Dealt data is smaller compared with camera.
Speedometer 	*Speed	The module made of Arduino Uno R3 *Angle of rotation of a wheel is obtained from Rotary encoder.
LRF 	*Obstacle *quick collision avoidance *Flag's pole	HOKUYO UTM-30LX & URG-04LX-UG01 *Angular range : 270 / 240 deg *Angular resolution : 0.25 / 0.352 deg
Omni directional camera 	*Lane *Pothole *Obstacles *Flag's color	SONY CCD EVI-370 with Hyperbolic mirror *Acquires 360 deg image *Image resolution provided 640 × 380
D-GPS 	*Pose	Hemisphere A100 *Horizontal accuracy : 0.6 m (DGPS mode) *Output rate : 20 Hz
fiber optic gyroscope 	*Angle	Japan Aviation Electronics Industry JG-35FD *Angular speed : 200 deg / s *Response frequency : 20 Hz / s

## 5. Software

### 5.1 Collision avoidance system

To safely avoid obstacles, we used the LRF to define a scanning area as shown in Fig. 8. The scanning area

consists of three areas: left, right, and front. The angle range of the left and right areas is  $45^\circ$ , while that of the front area is  $90^\circ$ . In all areas, the maximum detection distance of obstacles is set to 0.5 m (even when an emergency stop is executed). Our proposed module executes a different action depending on the area in which an obstacle is detected. When an obstacle is detected in the front area, the vehicle stops immediately to determine whether the

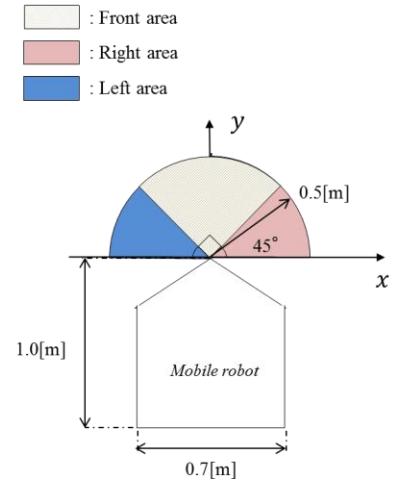


Fig. 8 Detection area

obstacle is static or dynamic. If the obstacle has not moved after a certain period, the vehicle performs a zero-radius turn, which depends on the direction of the detected obstacle.

When an obstacle is detected in the right (left) area, the vehicle performs a zero-radius turn and rotates counterclockwise (clockwise). When obstacles are detected simultaneously in more than one area, the vehicle stops immediately and waits for a certain period to determine whether the obstacles are static or dynamic. To prevent the obstacle avoidance system from entering a loop, the proposed module counts the number of areas in which an obstacle is detected. When the number of areas counted exceeds a predetermined threshold, the vehicle performs a zero-radius turn and rotates counterclockwise or clockwise depending on the direction of detected areas. When no obstacles are detected, the count number is reset.

### 5.2 JAUS

We developed a new Arduino-based JAUS protocol converter for each sensor and converted last year's conventional vehicle into a JAUS-compliant vehicle. The Arduino board with the Ethernet shield, through its Ethernet UDP connection, converts the protocols of various types of sensors, such as USB and/or RS232-based sensor, into the JAUS protocol. Currently, the GPS, gyroscope, and LRF sensors are JAUS-compliant sensor modules. Fig. 9 shows the developed

J AUS-compliant sensor module.

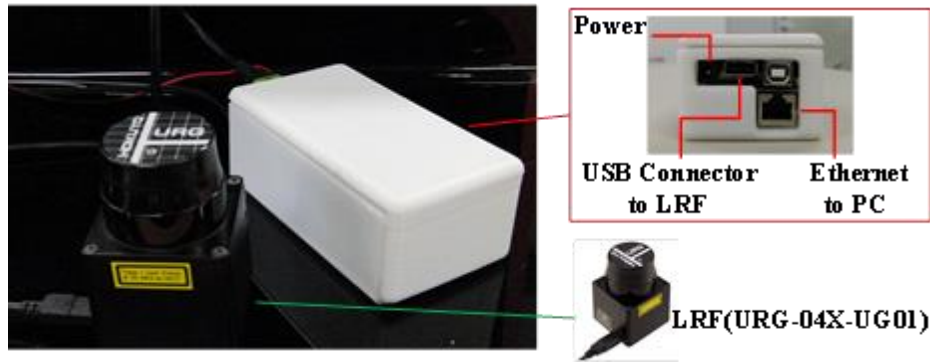


**Fig. 9 JAUS-compliant sensor module**

### 5.3 Lane detection

To track the sinusoidal curve in the Auto-Nav basic/advanced courses, we introduced a robust lane detection algorithm. In contrast to the straight-line approximation used last year, this algorithm uses lane interpolation and detects both straight and curved lanes. In Fig. 10, we illustrate the differences between images processed using last year and this year's algorithm.



**Fig. 10 (a) Processed image**

**using the new lane detection algorithm**

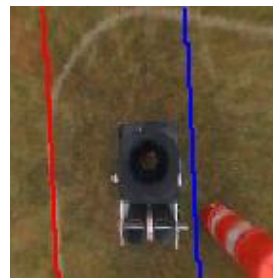


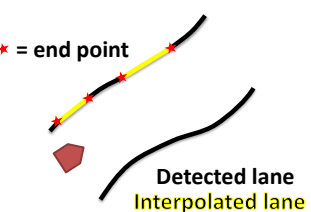
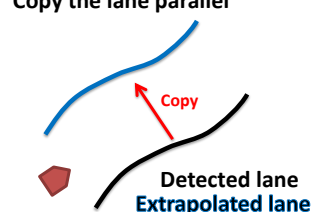
**Fig. 10 (b) Processed image**

**using last year's lane detection algorithm**

Figs. 11 (a)–(e) depict the basic procedure followed for image processing. Fig. 11 (a) shows an image captured by the omnidirectional camera. Fig. 11 (b) shows the reconstructed ground image. After reconstruction, the RGB color image is converted into a grayscale image using only the B component. Fig. 11 (c) shows the grayscale image. By using a referenced

lane template image prepared beforehand, we apply normalized template matching to detect lanes. This technique is robust to noise and sensitive to lanes. The template-matched image is converted into a binary image by comparing predetermined thresholds. Fig. 11 (d) shows the binary image. The algorithms of labeling and morphological thinning processes remove the isolated noise in the binary image; this process is called logical filtering. Fig. 11 (e) shows the logically filtered image. To detect lanes robustly, we applied a new spatial–temporal lane detection algorithm. Specifically, we combined the two types of lane detection algorithms presented in Table 5.

**Table 5. Roles of individual algorithms used into our new spatial–temporal lane detection algorithm**

<p style="text-align: center;"><b>Spatial lane detection</b></p>	<p>Lane interpolation based on piecewise lane images detected. Used to identify spatial relations among lane segments.</p>	<p>Connect the pair of end point</p> <p>* = end point</p>  <p>Detected lane Interpolated lane</p>
<p style="text-align: center;"><b>Temporal lane detection</b></p>	<p>Lane extrapolation based on historical knowledge of detected lanes. Used to identify historical relations among lane segments.</p>	<p>Copy the lane parallel</p>  <p>Detected lane Extrapolated lane</p>

In Fig. 11 (f1), we show typical lane-interpolation results obtained using only the spatial lane detection algorithm. In Fig. 11 (f2), we show typical lane-extrapolation results obtained using only the temporal lane detection algorithm. To achieve robust lane detection, we employ different lane detection algorithms depending on the properties of the input image.

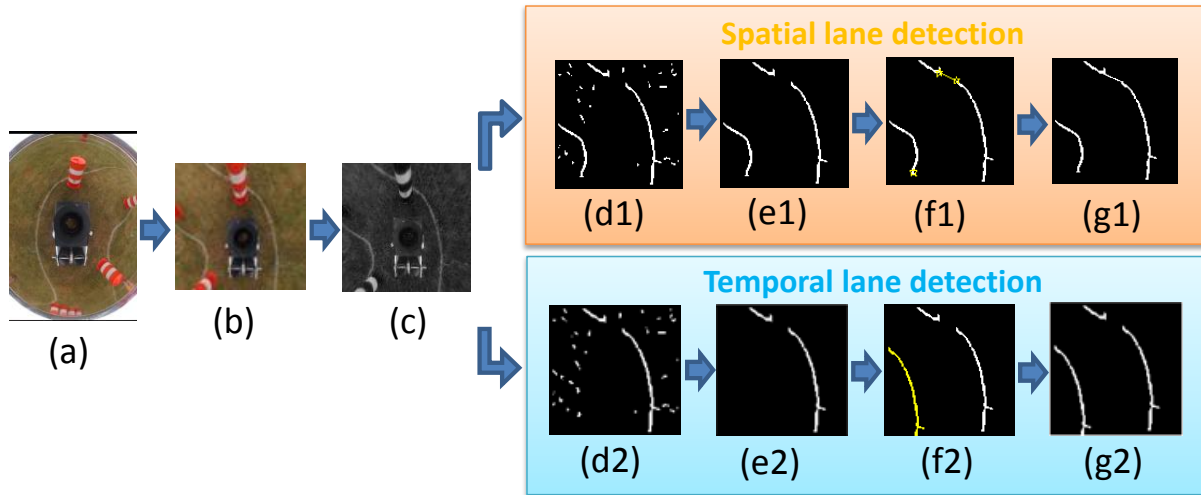
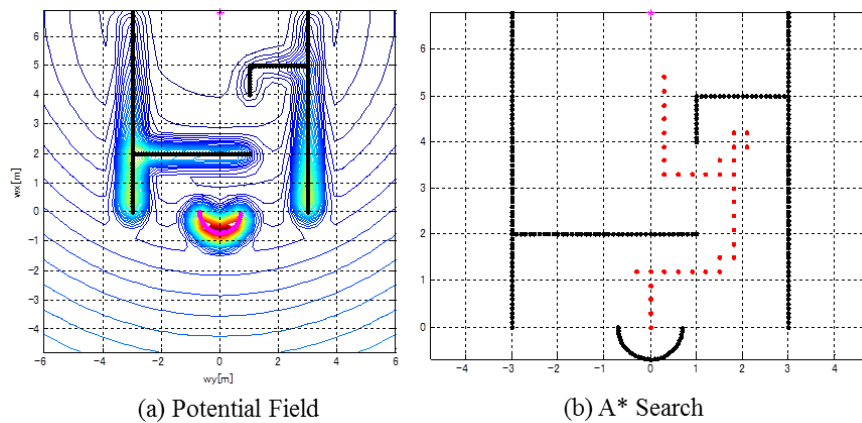
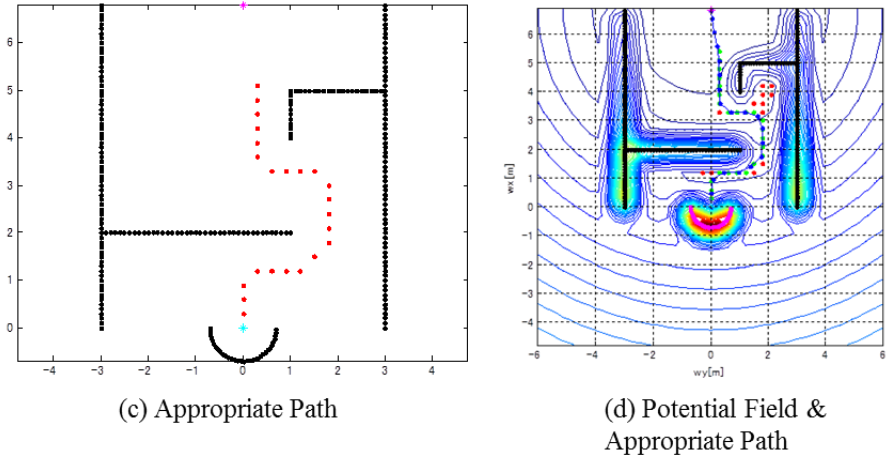


Fig.11 Lane detection results obtained using different lane detection algorithms

## 5.4 Path planning

To achieve robust and stable path planning for the vehicle, we combine two different path planning algorithms. In the first stage, we use LRF data and lines detected from the omnidirectional camera to generate a potential field map, as shown in Fig. 12 (a). In the second stage, we use the A-star search algorithm to generate the path for the vehicle. To prevent redundant search, when we detect a dead end in the potential field map, we increment the values of the potential field corresponding to the dead end, as shown in Fig. 12 (b). After iterating the first and second stages, we obtain a safe and minimum-distance path from the current position to the next waypoint, as shown in Fig. 12 (c). In Fig. 12 (d), we present the path obtained using our proposed path planning algorithm.





**Fig. 12 Overview of the path planning algorithm**

### 5.5 Map memorization

In the 2012 IGVC, during the Auto-Nav challenge, when our vehicle moved at relatively high speeds, it could not detect lines at steep curves. Consequently, our vehicle was charged with multiple internal-line crossing violations.

To decrease processing time, we utilize a global memorized map that is generated from historical lines and obstacle locations. In Fig. 13 (a), we present a snapshot of memorized lines and obstacle locations obtained from the actual 2012 IGVC course. Blue lines indicate memorized lines, while the red star marks indicate detected obstacles. Utilizing this global memorized map, we do not need to consume processing time for image processing to navigate through an unknown driving course, as shown in Figs. 13 (b) and (c).

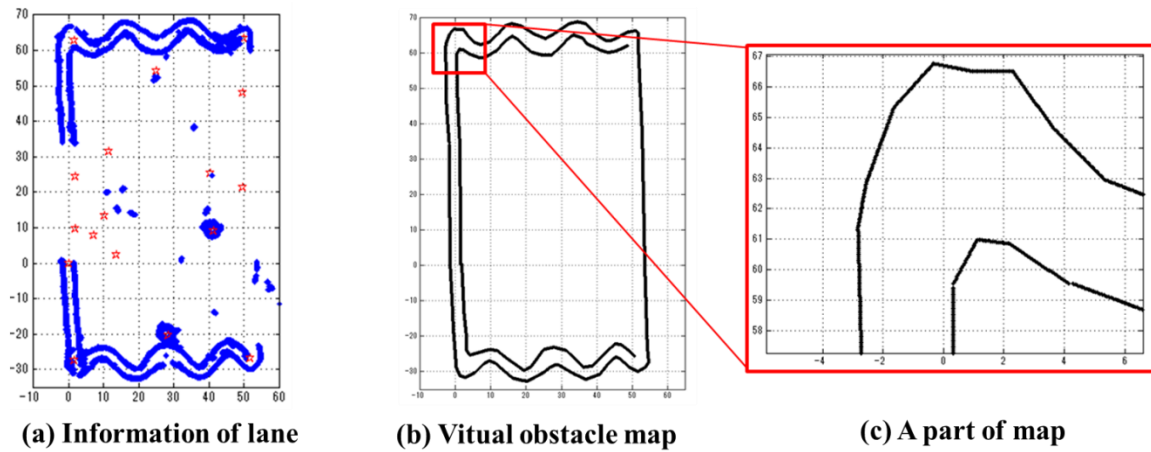


**Fig. 13 Depiction of global memorized map**

## 6. Performance

In Table 6, we compare the performance of last year's vehicle and the predicted performance of this year's vehicle. Most performance results of this year's vehicle are better than those of last year's vehicle. Moreover, the predicted performance results of this year's vehicle are in agreement with actual experimental results.

**Table 6. Performance comparison**

Measurement	Last year's vehicle	Performance prediction	Performance result
Speed	3.5mph(5.6km/h)	4.1 mph(6.5km/h)	3.7 mph(5.9km/h)
Ramp climbing ability	9.8-degree incline	10-degrees incline	10.2-degrees incline
Reaction time	0.45 seconds	0.3 seconds	0.35 seconds
Battery life	2 hours	3 hours	2 hours 20 minutes
Obstacle detection distance	0 to 10 m	0 to 10 m	0 to 10 m
Waypoint navigation	$\pm 0.14$ m	$\pm 0.10$ m	$\pm 0.14$ m

### 6.1 Speed

Because the center of gravity of this year's vehicle is lower than that of last year's vehicle, we can achieve a maximum speed (4.1 mph) according to the specifications of YAMAHA JW-Active.

### 6.2 Ramp climbing ability

Similar to Section 7.1, the ramp climbing ability of this year's vehicle is improved compared to that of last year's vehicle.

### 6.3 Reaction time

Due to safety reasons, we enforce two different reaction times. The first is used for normal reactions executed by the laptop computer. In these cases, it takes approximately 0.3–0.4 s to control the vehicle. The second is used by the emergency avoidance system. In the event of an emergence reaction, it takes approximately 0.2 s to control the vehicle. If an emergency stop occurs while the vehicle is moving at its maximum speed of 3.7 mph, the vehicle will travel approximately 0.5 m before stopping.

### 6.4 Battery

The capacity of the battery is 6.7 Ah. During use, the battery remains fully charged for approximately 3 h.

## 6.5 Evaluation of positioning accuracy during waypoint navigation

The standard deviation of the D-GPS, which has a navigation error less than  $\pm 0.14$  m, limits the accuracy by which Orange2013 can visit navigation waypoints.

## 7. Cost

Table 7 shows the costs incurred to develop Orange2013.

**Table 7. Estimated development costs for Orange2013**

Components	Retail Cost	Team Cost	Description
YAMAHA JW-Active	\$5,600	\$0	Electric wheelchair
HOKUYO UTM-30LX	\$4,000	\$0	Laser range finder
URG-04LX-UG01	\$909	\$909	Laser range finder
SONY EVI-370	\$360	\$0	CCD camera
Hyperbolic mirror	\$4,600	\$0	
I-O DATA GV-USB2	\$50	\$0	USB video capture cable
Japan Aviation Electronics Industry JG-35FD	\$5,800	\$0	Fiber optic gyroscope
Hemisphere A100	\$2,414	\$0	DGPS
FUJITSULIFEBOOK A561/C	\$1,000	\$0	Laptop personal computer
Mechanical parts	\$463	\$463	Various mechanical components
Electronic parts	\$248	\$248	Various electrical components
Total	\$25,444	\$1620	

## 8. Conclusion

In this report, we present the design and implementation of Orange2013 and describe how we used the FMECA design process to address hardware and software problems identified in last year's vehicle. Moreover, to adapt to the new rule changes in the 2013 IGVC, we developed a robust and reliable robotic system utilizing a 3D LRF module, collision avoidance system, and new lane detection algorithm. These capabilities aim in improving the safety, reliability, and durability of the vehicle. Consequently, we look forward to a favorable placement of Orange2013 in this year's IGVC competition.